

Crystal Structures and Magnetic Properties of Novel μ -Carboxylato- μ -Hydroxo-Bridged Binuclear Copper(II) Complexes with 1,10-Phenanthroline

Tadashi TOKII,* Naohiko HAMAMURA, Michio NAKASHIMA, and Yoneichiro MUTO
Department of Chemistry, Faculty of Science and Engineering, Saga University, Saga 840
(Received October 17, 1991)

Novel μ -carboxylato- μ -hydroxo-bridged binuclear copper(II) complexes with 1,10-phenanthroline, $[\text{Cu}_2(\text{OH})(\text{RCOO})(\text{phen})_2]\text{X}_2 \cdot \text{H}_2\text{O}$ (where $\text{R}=\text{H}$, $\text{X}=\text{BF}_4$ (**1**); $\text{R}=\text{CH}_3$, $\text{X}=\text{NO}_3$ (**2**); $\text{R}=\text{C}_2\text{H}_5$, $\text{X}=\text{NO}_3$ (**3**)) were prepared and characterized by elemental analyses, electronic spectra, magnetic susceptibilities, and X-ray structure analysis. The magnetic susceptibility data conform to the usual dimer equation. The $-2J$ values are -109 cm^{-1} for **1**, -111 cm^{-1} for **2**, and -109 cm^{-1} for **3**, indicating that a strong ferromagnetic spin coupling exists in these complexes. The crystal structures of **2** and **3** were determined by the single-crystal X-ray diffraction method. The crystallographic data are: Compound **2**, monoclinic, $P2_1/n$, $a=8.107$ (10), $b=18.554$ (9), $c=18.616$ (7) Å, $\beta=99.14$ (6)°, $V=2765$ (6) Å³, $Z=4$, $R=0.045$ for 3274 observed unique reflections; compound **3**, monoclinic, $P2_1/n$, $a=7.981$ (10), $b=18.352$ (8), $c=19.247$ (8) Å, $\beta=97.98$ (7)°, $V=2792$ (4) Å³, $Z=4$, $R=0.047$ for 3220 reflections. These complexes have very novel roof-shaped binuclear units with dihedral angles (122.8° for **2** and 122.7° for **3**) observed between two basal planes of CuO_2N_2 . These small dihedral angles are mainly attributed to the strong ferromagnetic exchange interaction in the present complexes.

μ -Hydroxo- or μ -alkoxo-bridged copper(II) complexes have been extensively studied. Hatfield and Hodgson established a linear correlation between the values of $-2J$ (singlet–triplet energy separation) and of the Cu–O–Cu bridging angle (ϕ). The $-2J$ value increases with increasing ϕ ($-2J/\text{cm}^{-1} = -74.5\phi/\text{deg} + 7270$).¹⁾ This result has been rationalized in terms of an orbital model developed by Hoffmann and co-workers.²⁾ In several cases, however, the $-2J$ value is much smaller than that expected from its large ϕ . To explain this contradiction, the following two effects have been proposed separately: (i) a bending effect between two basal planes containing each copper(II) ion,^{3,4)} and (ii) an orbital countercomplementary effect.⁵⁾ Summarizing the substance of this effect, the weaker observed anti-ferromagnetic interaction in copper(II) dimers with a set of two different bridging groups results from competition between two different magnetic exchange pathways, which may have opposite phases relative to each other. In recent papers, we have described both the magnetic properties and the crystal structures of di- μ -carboxylato-bridged binuclear copper(II) complexes with 1,10-phenanthroline, $[\text{Cu}(\text{RCOO})(\text{phen})(\text{H}_2\text{O})]_2(\text{NO}_3)_2 \cdot 4\text{H}_2\text{O}$.⁶⁾ As a part of continuing projects in this study, we have prepared novel roof-shaped μ -carboxylato- μ -hydroxo-bridged binuclear copper(II) complexes with phen, $[\text{Cu}_2(\text{OH})(\text{RCOO})(\text{phen})_2]\text{X}_2 \cdot \text{H}_2\text{O}$. Here, we report on the preparation, crystal structures, and magnetic properties of these complexes. Based on our results, we investigated the following three factors: The Cu–O–Cu bridging angle, the bending effect, and the orbital countercomplementary effect that may be cooperatively responsible for the magnetic interactions between copper(II) ions in the copper(II) dimers with two different bridging groups.

Experimental

Syntheses. Compound **1**: Formic acid (10 mmol) and 1,10-phenanthroline (10 mmol) were dissolved in 50 cm³ of water; the resulting solution was adjusted to pH 5.0 with 1 mol dm⁻³ aqueous NaOH. To this solution 10 mmol of 45% aqueous $\text{Cu}(\text{BF}_4)_2$ was added under stirring; the pH was then adjusted to 4.0. Earlier precipitates were filtered off, and the filtrate was concentrated to one third of its volume. Blue precipitates were collected, washed with water, and air-dried at room temperature. Found: C, 40.33; H, 2.77; N, 7.53; Cu, 17.16%. Calcd for $\text{C}_{25}\text{H}_{20}\text{B}_2\text{Cu}_2\text{F}_8\text{N}_4\text{O}_4$: C, 40.51; H, 2.72; N, 7.56; Cu, 17.15%.

Compound **2**: Acetic acid (10 mmol) and 1,10-phenanthroline (10 mmol) were dissolved in 15 cm³ of methanol. To this solution 10 cm³ of 1 mol dm⁻³ aqueous CuX_2 was added under stirring; the resulting solution was adjusted to pH 4.0 with 1 mol dm⁻³ aqueous NaOH. Earlier precipitates were filtered off, and the filtrate was allowed to stand overnight at room temperature. The precipitated deep-blue crystals were collected, washed with water, and air-dried. Found: C, 44.07; H, 3.07; N, 11.83; Cu, 17.90%. Calcd for $\text{C}_{13}\text{H}_{11}\text{CuN}_3\text{O}_5$: C, 44.26; H, 3.14; N, 11.91; Cu, 18.01%.

Compound **3**: The complex was obtained as deep-blue prisms in the same way as that of compound **2**, except for using propionic acid instead of acetic acid. Found: C, 45.07; H, 3.42; N, 11.70; Cu, 17.54%. Calcd for $\text{C}_{27}\text{H}_{24}\text{Cu}_2\text{N}_6\text{O}_{10}$: C, 45.06; H, 3.36; N, 11.68; Cu, 17.66%.

Physical Measurements. The magnetic susceptibilities were determined by the Faraday method in the 80–300 K temperature range. The effective magnetic moments per copper ion at room temperature were calculated using

$$\mu_{\text{eff}} = 2.83\sqrt{(\chi_A - N\alpha)T},$$

where χ_A is the molar magnetic susceptibility corrected for the diamagnetism of the constituent atoms using Pascal's constant;⁷⁾ $N\alpha$ is the temperature-independent paramagnetism per mole of copper(II). The value of $N\alpha$ was assumed to be

$60 \times 10^{-6} \text{ emu mol}^{-1}$ ($1 \text{ emu} = 4\pi \times 10^{-6} \text{ m}^3$). The observed magnetic susceptibility data were fitted to Eq. 1. The best-fit parameters of $-2J$ and g were obtained by a nonlinear least-squares fitting procedure. The quantity of the fit was estimated by means of a discrepancy index,

$$\sigma_{\text{dis}} = \left[\frac{\sum (\chi_{\text{obsd}} - \chi_{\text{calcd}})^2}{\sum \chi_{\text{obsd}}^2} \right]^{1/2}.$$

The magnetic data are given in Table 4 and are represented graphically in Fig 3.

The electronic spectra of all the complexes investigated were recorded by a diffuse reflectance technique with a Hitachi 323 recording spectrophotometer.

X-Ray Crystal Structure Determination. The diffraction data were measured on a Rigaku AFC5S automated four-circle diffractometer with graphite monochromated Cu $K\alpha$ radiation ($\lambda = 1.54178 \text{ \AA}$) at $23 \pm 1^\circ \text{C}$. The unit-cell parameters of each crystal were obtained from a least-squares refinement based on 25 high-angle reflections. The crystal data are given in Table 1. The data were collected at a temperature of $23 \pm 1^\circ \text{C}$ using the ω - 2θ scan technique to a maximum 2θ value of 120° . The weak reflections ($I < 10\sigma(I)$) were rescanned (maximum of 2 rescans) and the counts were accumulated in order to assure good counting statistics. Stationary background counts were recorded on each side of the reflection. The ratio of the peak counting time to the background counting time was 2:1. The intensities of three representative reflections, which were measured after every 150 reflections, remained constant throughout data collection, indicating crystal and electronic stability (no decay correction was applied).

An empirical absorption correction based on azimuthal scans of several reflections was applied which resulted in transmission factors ranging from 0.81 to 1.00 for **2** and from 0.70 to 1.00 for **3**. The data were corrected for Lorentz and polarization effects.

The structure was solved by direct methods.⁸⁾ The non-

hydrogen atoms were refined anisotropically. Refinements were carried out by the full-matrix least-squares method.⁹⁾ All of the hydrogen atoms were located from the subsequent difference Fourier maps and included in the refinement. The final discrepancy factors,

$$R = \sum ||F_o| - |F_c|| / \sum |F_o|$$

and

$$R_w = [(\sum w(|F_o| - |F_c|)^2) / \sum w F_o^2]^{1/2},$$

are listed in Table 1.

The neutral-atom scattering factors were taken from Cromer and Waber.¹⁰⁾ Anomalous dispersion effects were included in F_{calcd} ; the values for $\Delta f'$ and $\Delta f''$ were those of Cromer.¹⁰⁾ All calculations were performed using the TEXSAN¹¹⁾ crystallographic software package of Molecular Structure Corporation. The final positional and thermal parameters along with their estimated standard deviations are given in Table 2. The coordinates and isotropic temperature factors of the hydrogen atoms, the anisotropic thermal parameters of nonhydrogen atoms, and the $F_o - F_c$ tables have been deposited as Document No. 8987 at the Chemical Society of Japan.

Results and Discussion

Crystal Structure. X-Ray structure analyses of **2** and **3** revealed that two copper atoms are linked by hydroxo and carboxylato bridges with separations of 3.017 (2) and 3.015 (2) \AA , respectively (Figs. 1 and 2). The selected bond lengths and angles for **2** and **3** are listed in Table 3. These are very novel structures, having both μ -carboxylato and μ -hydroxo bridges.^{12,13)} The Cu...Cu distances are somewhat longer than those in di- μ -hydroxo-bridged copper(II) dimers (2.85–3.00 \AA).¹⁴⁾ The coordination geometry of each copper atom is essentially square planar with one hydroxo-oxygen, one of the carboxylato-oxygens, and two nitrogen donors of

Table 1. Crystallographic Data for Compounds **2** and **3**

	2	3
Formula	$\text{C}_{26}\text{H}_{22}\text{Cu}_2\text{N}_6\text{O}_{10}$	$\text{C}_{27}\text{H}_{24}\text{Cu}_2\text{N}_6\text{O}_{10}$
F_w	705.59	719.61
Crystal dimensions (mm)	0.40×0.40×0.80	0.20×0.10×0.30
Crystal system	Monoclinic	Monoclinic
Space group	$P2_1/n$	$P2_1/n$
$a/\text{\AA}$	8.107 (10)	7.981 (10)
$b/\text{\AA}$	18.554 (9)	18.352 (8)
$c/\text{\AA}$	18.616 (7)	19.247 (8)
β/deg	99.14 (6)	97.98 (7)
$V/\text{\AA}^3$	2765 (6)	2792 (4)
Z	4	4
$D_c/\text{g cm}^{-3}$	1.695	1.683
$D_m/\text{g cm}^{-3}$	1.69	1.69
$F(000)$	1432	1440
$\mu(\text{Cu } K\alpha)/\text{cm}^{-1}$	24.60	24.37
No. of Observations ($F_o > 3.00\sigma(F_o)$)	3274	3220
No. of variables	397	406
Residuals		
R	0.045	0.047
R_w	0.059	0.069
Largest Peak in Final Diff. Fourier ($e/\text{\AA}^3$)	0.81	1.09

Table 2. Fractional Coordinates ($\times 10^4$) and Equivalent Isotropic Thermal Parameters

Atom	x	y	z	$B_{eq}/\text{\AA}^2$	Atom	x	y	z	$B_{eq}/\text{\AA}^2$
Compound 2					Compound 3				
Cu1	3446.7(9)	1932.7(3)	7064.7(3)	3.59(3)	Cu1	8360(1)	1879.9(4)	7138.1(4)	2.96(3)
Cu2	3423.3(9)	332.6(3)	7350.3(3)	3.68(3)	Cu2	8257(1)	276.0(4)	7468.0(4)	3.07(3)
O1	2168(4)	1196(2)	7451(2)	3.8(1)	O1	7021(4)	1163(2)	7534(2)	3.1(1)
O2	3109(4)	1550(2)	6087(2)	4.3(2)	O2	8079(5)	1456(2)	6206(2)	3.7(2)
O3	3183(4)	361(2)	6300(2)	4.2(1)	O3	8028(5)	267(2)	6453(2)	3.6(2)
O4	5664(4)	1144(2)	7491(2)	4.3(1)	O4	10572(5)	1088(2)	7538(2)	4.0(2)
O5	9872(7)	1859(3)	9204(3)	10.6(3)	O5	3502(6)	1198(3)	6784(2)	5.6(2)
O6	7290(7)	1847(3)	8795(3)	9.0(3)	O6	3730(10)	1096(4)	5706(3)	11.5(5)
O7	8620(10)	909(3)	8818(4)	11.8(4)	O7	1649(9)	657(5)	6130(4)	12.9(5)
O8	3537(6)	3792(2)	1793(2)	6.5(2)	O8	2196(8)	1902(3)	8765(3)	8.6(3)
O9	4155(7)	3988(3)	740(3)	9.3(3)	O9	3500(10)	910(4)	8719(4)	9.5(4)
O10	1807(8)	3925(6)	891(5)	21.6(8)	O10	4773(7)	1818(3)	9256(3)	8.2(3)
N1	3547(5)	2568(2)	7952(2)	3.6(2)	N1	8485(5)	2539(2)	7983(2)	3.0(2)
N2	4603(5)	2790(2)	6702(2)	3.6(2)	N2	9514(5)	2737(2)	6757(2)	3.2(2)
N3	4631(5)	-625(2)	7331(2)	4.0(2)	N3	9459(5)	-694(2)	7480(2)	3.3(2)
N4	3294(5)	2(2)	8378(2)	4.0(2)	N4	8138(6)	-3(2)	8473(2)	3.4(2)
N5	8629(7)	1543(3)	8944(3)	5.6(3)	N5	2960(7)	1051(3)	6174(3)	4.5(2)
N6	3137(7)	3903(2)	1119(3)	5.3(2)	N6	3516(8)	1554(3)	8916(3)	5.0(3)
C1	3075(6)	904(3)	5885(3)	4.0(2)	C1	7963(7)	797(3)	6040(3)	3.2(2)
C2	2914(8)	765(3)	5085(3)	5.9(3)	C2	7721(8)	601(3)	5266(3)	4.2(3)
C3	2990(7)	2446(3)	8567(3)	4.8(2)	C3	8230(10)	1205(4)	4791(3)	5.6(3)
C4	3098(7)	2950(3)	9127(3)	5.0(3)	C4	7951(7)	2427(3)	8592(3)	3.9(2)
C5	3766(7)	3616(3)	9034(3)	4.6(2)	C5	8088(8)	2936(3)	9128(3)	4.1(3)
C6	4362(6)	3769(2)	8386(3)	3.8(2)	C6	8840(7)	3592(3)	9029(3)	4.0(2)
C7	5064(7)	4451(3)	8222(3)	4.5(2)	C7	9429(7)	3743(3)	8388(3)	3.4(2)
C8	5577(7)	4572(3)	7578(3)	4.6(2)	C8	10176(7)	4417(3)	8217(3)	3.9(2)
C9	5471(6)	4014(2)	7032(3)	3.9(2)	C9	10661(7)	4525(3)	7574(3)	3.9(2)
C10	5975(7)	4098(3)	6355(3)	4.8(2)	C10	10466(7)	3977(3)	7058(3)	3.3(2)
C11	5780(7)	3530(3)	5870(3)	5.0(3)	C11	10925(8)	4044(3)	6383(3)	4.2(3)
C12	5098(7)	2887(3)	6056(3)	4.3(2)	C12	10694(8)	3475(3)	5917(3)	4.4(3)
C13	4787(6)	3348(2)	7185(2)	3.4(2)	C13	9965(8)	2825(3)	6121(3)	4.1(2)
C14	4228(6)	3228(2)	7859(2)	3.4(2)	C14	9752(6)	3302(3)	7216(3)	3.1(2)
C15	5268(7)	-922(3)	6789(3)	4.8(2)	C15	9211(6)	3189(2)	7885(3)	2.9(2)
C16	5915(7)	-1621(3)	6837(3)	5.8(3)	C16	10093(7)	-1025(3)	6961(3)	3.7(2)
C17	5891(7)	-2023(3)	7449(4)	6.0(3)	C17	10793(8)	-1723(3)	7038(3)	4.4(3)
C18	5215(7)	-1725(3)	8034(3)	5.0(2)	C18	10783(7)	-2102(3)	7650(4)	4.5(3)
C19	5105(8)	-2088(3)	8713(4)	6.5(3)	C19	10112(7)	-1759(3)	8215(3)	3.7(2)
C20	4465(8)	-1762(3)	9244(4)	6.1(3)	C20	10051(8)	-2090(3)	8881(4)	5.0(3)
C21	3871(7)	-1032(3)	9178(3)	5.0(3)	C21	9432(8)	-1729(4)	9405(4)	5.0(3)
C22	3191(8)	-656(4)	9707(3)	5.9(3)	C22	8806(8)	-1006(3)	9302(3)	4.3(3)
C23	2531(8)	10(4)	9588(3)	6.1(3)	C23	8100(10)	-589(4)	9804(3)	5.1(3)
C24	2593(8)	326(3)	8881(3)	5.1(3)	C24	7420(10)	69(4)	9627(3)	5.2(3)
C25	3924(6)	-673(2)	8514(3)	3.9(2)	C25	7436(8)	353(3)	8961(3)	4.3(3)
C26	4621(6)	-1013(2)	7947(3)	4.1(2)	C26	8806(7)	-677(3)	8637(3)	3.3(2)
					C27	9497(7)	-1056(3)	8101(3)	3.2(2)

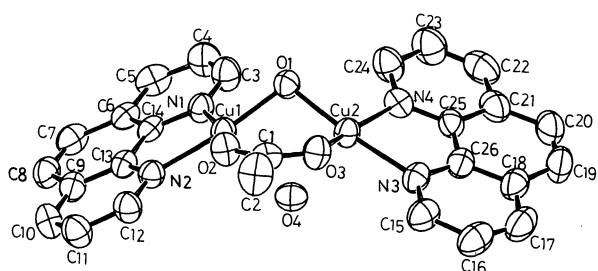


Fig. 1. ORTEP drawing for the complex cation of 2 with thermal ellipsoids scaled at the 50% probability level. Hydrogen atoms and NO_3^- have been omitted for clarity.

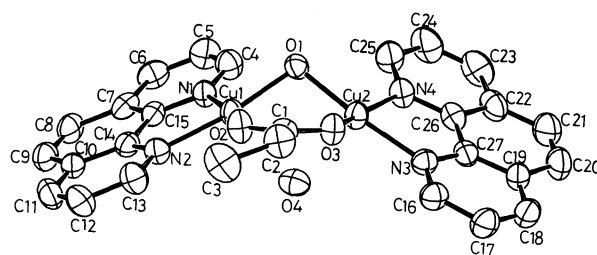


Fig. 2. ORTEP drawing for the complex cation of 3 with thermal ellipsoids scaled at the 50% probability level.

Table 3. Selected Bond Lengths (Å) and Angles (°)

	2	3
Cu1...Cu2	3.017(2)	3.015(2)
Cu1-O1	1.922(3)	1.918(3)
Cu1-O2	1.933(3)	1.939(4)
Cu1-N1	2.021(4)	2.018(4)
Cu1-N2	2.017(4)	2.012(4)
Cu2-O1	1.923(3)	1.917(3)
Cu2-O3	1.935(3)	1.936(4)
Cu2-N3	2.031(4)	2.021(4)
Cu2-N4	2.027(4)	2.015(4)
Cu1...O4	2.356(4)	2.333(4)
Cu2...O4	2.342(4)	2.363(4)
Cu1-O1-Cu2	103.4(2)	103.6(2)
O1-Cu1-N2	173.2(1)	171.7(2)
O1-Cu1-N1	93.6(1)	93.4(2)
O1-Cu1-O2	95.0(1)	95.4(2)
O2-Cu1-N1	165.0(1)	166.4(2)
O2-Cu1-N2	88.7(1)	88.6(2)
N1-Cu1-N2	81.6(2)	81.5(2)
O1-Cu2-N3	173.9(1)	174.4(2)
O1-Cu2-N4	93.0(2)	93.4(2)
O1-Cu2-O3	96.1(1)	95.6(1)
O3-Cu2-N4	161.8(1)	162.8(2)
O3-Cu2-N3	88.7(1)	89.0(2)
N3-Cu2-N4	81.4(2)	81.4(2)
Cu1-O2-C1	128.7(3)	128.2(3)
Cu2-O3-C1	128.7(3)	128.6(3)
O2-C1-O3	125.6(4)	126.4(5)

phen. Each copper atom has an additional weak interaction with the third oxygen atom O4(H₂O), forming an almost symmetrical bridge. However, these linkages are much weaker, since the Cu-O4 distances (2.33–2.36 Å) are noticeably longer than the basal Cu-O bond distances (1.92–1.94 Å). Each copper atom deviates slightly from the basal plane. The mean values of the deviation are 0.15 Å for **2** and 0.14 Å for **3**. An elongation of the Cu...Cu distance is reflected in a simultaneous opening of the Cu-O1-Cu bridging angle. The Cu-O1-Cu bridging angles are 103.4 (2)° for **2** and 103.6 (2)° for **3**, corresponding to the maximum value of those found in di- μ -hydroxo-bridged copper(II) complexes, which range from 95.6 to 104.1°. The long Cu...Cu distances are also reflected in the Cu-O-C angles of the carboxylato ions in the present complexes. These angles have average values of 128.7° for **2** and 128.4° for **3**, about 5° greater than those found in binuclear copper(II) carboxylates.¹⁴ The Cu-O-C angles, however, are nearly equal to those observed for di- μ -carboxylato-bridged copper(II) dimers.^{6,15} The most interesting and unusual feature of the structure in **2** and **3** is the dihedral angle (δ) observed between the best least-squares planes through the two copper coordination spheres, (Cu1, O1, O2, N1, and N2) and (Cu2, O1, O3, N3, and N4). The values of δ are equal to 122.8° for **2** and 122.7° for **3**, which are novel examples of such close angles, very different from 180°.

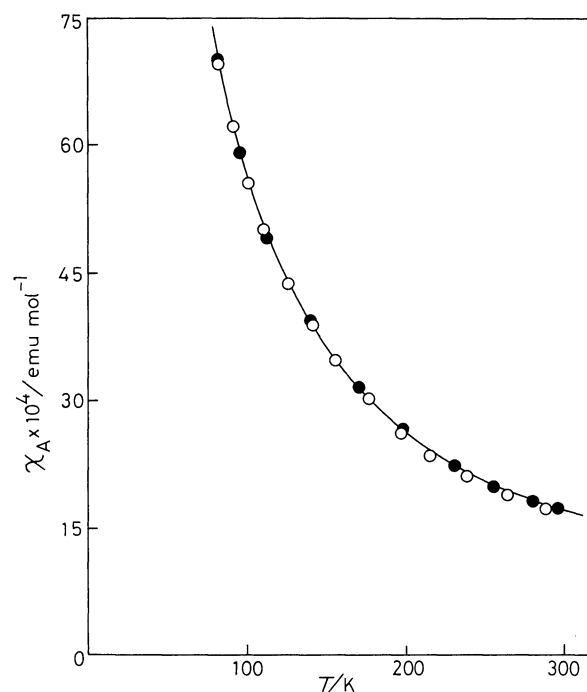


Fig. 3. Temperature dependence of magnetic susceptibilities for compounds **1** (●) and **2** (○). The solid curve was calculated from Eq. 1 using the following parameters: $-2J = -109 \text{ cm}^{-1}$ and $g = 2.18$.

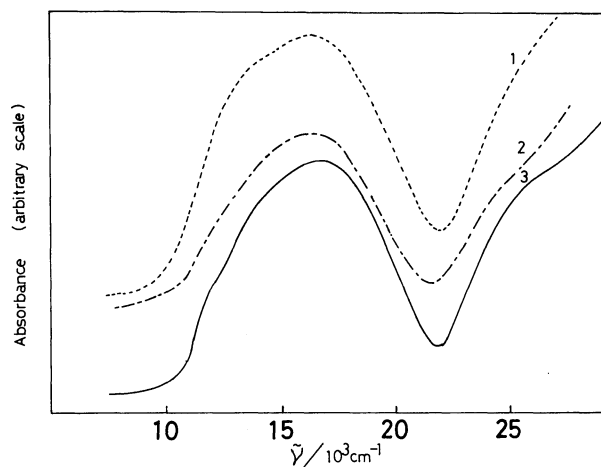


Fig. 4. Reflectance spectra of compounds **1**–**3**.

Electronic Spectra. The reflectance spectra of the present three complexes are very similar to one another in shape, giving a band maximum at ca. $16.8 \times 10^3 \text{ cm}^{-1}$ with a shoulder at ca. 13.5×10^3 (Fig. 4). These spectral patterns may be attributed to the square-planar configuration around the copper(II) ion with a weak perturbation from the fifth coordinating site.¹⁶ The spectral similarity suggests that compound **1** also has the same configuration as those in **2** and **3**.

Magnetic Susceptibilities. The magnetic susceptibilities of the complexes were determined over the temperature range of 80–300 K. The magnetic data for the

Table 4. Magnetic Data for $[\text{Cu}_2(\text{OH})(\text{RCOO})(\text{phen})_2]\text{X}_2 \cdot \text{H}_2\text{O}$

R	X	$-2J/\text{cm}^{-1}$	g	$\mu_{\text{eff}}/\text{B.M. (T/K)}$
H	BF_4	-109	2.18	1.98(295)
CH_3	NO_3	-111	2.17	1.96(288)
C_2H_5	NO_3	-109	2.19	1.98(290)

complexes are well represented by the well-known Bleaney-Bowers equation,¹⁷⁾

$$\chi_A = (Ng^2\beta^2/kT)[3 + \exp(-2J/kT)]^{-1} + N\alpha. \quad (1)$$

The best-fit parameters of $-2J$ and g were obtained by a nonlinear least-squares fitting procedure (Table 4). The $-2J$ values listed in Table 4 are almost the same in the range of -109 — -111 cm^{-1} range, indicating that strong ferromagnetic exchange interactions are operating in these complexes. We first notice that this magnetic behavior rules out an established fact concerning the order in the strength of the magnetic interaction in binuclear copper(II) carboxylates; formate bridges mediate stronger antiferromagnetic coupling than do those by acetato or propionato. The $-2J$ values of copper(II) formate complexes are about 1.5 times as large as those of copper(II) acetate or propionate complexes.^{6,18)} The equality in $-2J$ among the present complexes is presumably due to the small contribution of the additional carboxylato bridging ligand for the ferromagnetic interaction. Thus, the orbital countercomplementary effect on the magnetic interaction may not work or may not be noticeably different in the present complexes. Second, compounds **1**—**3** have a triplett ground state, whereas the bridging Cu—O—Cu angles are $103.4 (2)^\circ$ for **2** and $103.6 (2)^\circ$ for **3**. In planar di- μ -hydroxo-bridged binuclear copper(II) complexes, the slope of the plots of $-2J$ vs. bridging Cu—O—Cu angles is $-74.5 \text{ cm}^{-1} \text{ deg}^{-1}$ with $-2J=0$ for a bridge angle of 97.6° .¹⁾ If the data for compounds **2** and **3** fit onto the same correlation line, the exchange parameter ($-2J$) could be predicted to be 433 cm^{-1} for **2** and 448 cm^{-1} for **3**. However, values of -111 cm^{-1} for **2** and -109 cm^{-1} for **3** were, actually found. These values are very small, even when considering that the present complexes have one hydroxo-bridge. According to Kahn et al., the dihedral angle between the two basal planes containing each copper(II) ion has also been regarded as being an important factor in determining the strength of the magnetic interaction; the spin coupling become more ferromagnetic when the dihedral angle decreases from 180° to 130° .³⁾ In compounds **2** and **3**, the dihedral angles (122.8° and 122.7°) are close to 130° . Therefore, the ferromagnetic interaction observed for the present complexes is mainly attributed to the small dihedral angle.⁴⁾

Recently, Lippard et al. have prepared μ -acetato- μ -hydroxo-bridged binuclear copper(II) complex, $[\text{Cu}_2(\text{OH})(\text{CH}_3\text{COO})(\text{L})]^{2+}$ (L=hexaimidazole ligand), in

which the dihedral angle δ is 117.5° and the Cu—O—Cu angle ϕ is 109.3° . This complex shows a weak ferromagnetic interaction, $-2J=-2.6 \text{ cm}^{-1}$.¹²⁾ In this complex, the bridging angle (109.3°) is significantly larger than those of **2** and **3**, whereas the dihedral angle (117.5°) is noticeably smaller than those of **2** and **3**. These results suggest that the Cu—O—Cu bridging angle still plays an important role in the magnetic interaction, though the small dihedral angle mainly causes a strong ferromagnetic exchange interaction of roof-shaped complexes, such as possessed by the present complexes.

References

- 1) D. J. Hodgson, *Prog. Inorg. Chem.*, **19**, 173 (1975); Van H. Crawford, H. W. Richardson, J. R. Wasson, D. J. Hodgson, and W. E. Hatfield, *Inorg. Chem.*, **15**, 2107 (1976).
- 2) P. J. Hay, J. C. Thibault, and R. Hoffmann, *J. Am. Chem. Soc.*, **97**, 4884 (1975).
- 3) M. F. Charlot, S. Jeannin, Y. Jeannin, O. Kahn, J. L. Abaul, and J. M. Frere, *Inorg. Chem.*, **18**, 1675 (1979).
- 4) Y. Nishida, M. Masumoto, and Y. Mori, *Z. Naturforsch., B*, **44**, 307 (1989).
- 5) Y. Nishida, M. Takeuchi, K. Takahashi, and S. Kida, *Chem. Lett.*, **1985**, 631; Y. Nishida and S. Kida, *J. Chem. Soc., Dalton Trans.*, **1986**, 2633.
- 6) T. Tokii, N. Watanabe, M. Nakashima, Y. Muto, M. Morooka, S. Ohba, and Y. Saito, *Chem. Lett.*, **1989**, 1671; *Bull. Chem. Soc. Jpn.*, **63**, 364 (1990).
- 7) P. W. Selwood, "Magnetochemistry," Interscience Publishers, New York (1956), pp. 78 and 91.
- 8) Structure Solution Methods: MITHRIL
C. J. Gilmore; MITHRIL - an integrated direct methods computer program. *J. Appl. Cryst.*, **17**, 42 (1984).
DIRDIF
P. T. Beurskens; DIRDIF: Direct Methods for Difference Structures - an automatic procedure for phase extension and refinement of difference structure factors. Technical Report 1984/1 Crystallography Laboratory, Toernooiveld, 6525 Ed Nijmegen, Netherlands.
- 9) Least-Squares:
Function minimized: $\sum w(|F_o| - |F_c|)^2$,
where: $w = 4F_o^2/\sigma^2(F_o^2)$
Standard deviation of an observation of unit weight:
 $[\sum w(|F_o| - |F_c|)^2/(N_o - N_v)]^{1/2}$,
where: N_o =number of observations,
 N_v =number of variables.
- 10) D. T. Cromer and J. T. Waber, "International Tables for X-Ray Crystallography," The Kynoch Press, Birmingham, England(1974), Vol. IV.
- 11) TEXSAN-TEXRAY Structure Analysis Package, Molecular Structure Corporation (1985).
- 12) W. B. Tolman, R. L. Rardin, and S. J. Lippard, *J. Am. Chem. Soc.*, **111**, 4532 (1989).
- 13) G. Christou, S. P. Perlepes, E. Libby, K. Folting, J. C. Huffman, R. J. Webb, and D. N. Hendrickson, *Inorg. Chem.*, **29**, 3657 (1990).
- 14) M. Melnik, *Coord. Chem. Rev.*, **42**, 259 (1982), and references therein.

- 15) M. Mikuriya, S. Kida, I. Ueda, T. Tokii, and Y. Muto, *Bull. Chem. Soc. Jpn.*, **50**, 2464 (1977).
- 16) A. A. G. Tomlinson, B. J. Hathaway, D. E. Billing, and P. Nicholls, *J. Chem. Soc. A*, **1969**, 65.
- 17) B. Bleaney and K. D. Bowers, *Proc. R. Soc. London, Ser. A*, **214**, 451 (1952).
- 18) R. J. Doedens, *Prog. Inorg. Chem.*, **21**, 209 (1976); M. Kato and Y. Muto, *Coord. Chem. Rev.*, **92**, 45 (1988); M. Yamanaka, H. Uekusa, S. Ohba, Y. Saito, S. Iwata, M. Kato, T. Tokii, Y. Muto, and O. W. Steward, *Acta Crystallogr., Sect. B*, **47**, 344 (1991).
-